

Petrographic Characterization and Depositional Conditions of Surkha lignite from Saurashtra Basin, Western India

Vikram P. Singh*, Mahesh Shivanna, Bhagwan D. Singh and Alpana Singh

Birbal Sahni Institute of Palaeobotany, 53 University Road, Lucknow - 226 007

*Corresponding author's e-mail: vikramchauhan09@rediffmail.com

Manuscript received: 03 February 2016

Accepted for publication: 16 April 2016

ABSTRACT

Singh V. P., Shivanna M., Singh B. D. & Singh A. 2016. Petrographic Characterization and Depositional Conditions of Surkha lignite from Saurashtra Basin, Western India. *Geophytology* 46(1): 75-88.

A petrographic study has been carried out on Surkha lignite deposits (early Eocene) of Gujarat state to determine the maceral composition and to infer the depositional conditions. The quantitative petrographic analysis shows that there is dominance of huminite group of macerals over the liptinite and inertinite groups. Telohuminite (structured) and detrohuminite (detritus) submacerals mainly represent the huminite group of macerals. Ulminite dominates amongst the telohuminite macerals, while attrinite and densinite contribute to detrohuminite. The huminite reflectance values (R_r : 0.27-0.34%) indicate that the lignites are less mature and have reached up to the lignitic stage of coalification. Gelification and tissue preservation indices of lignites suggest that the precursor peat was generated mainly in the upper deltaic regime. Further, extrapolation of ground water and vegetation indices suggests that peat precursors of Surkha lignite were accumulated under mesotrophic to the rheotrophic hydrological regime. The studied lignite is comparable to the Khadsaliya lignite of the Saurashtra Basin in having similarities in overall petrographic characteristics and depositional conditions of lignites.

Key-words: Macerals, rank (maturity), depositional condition, Eocene lignite, Gujarat.

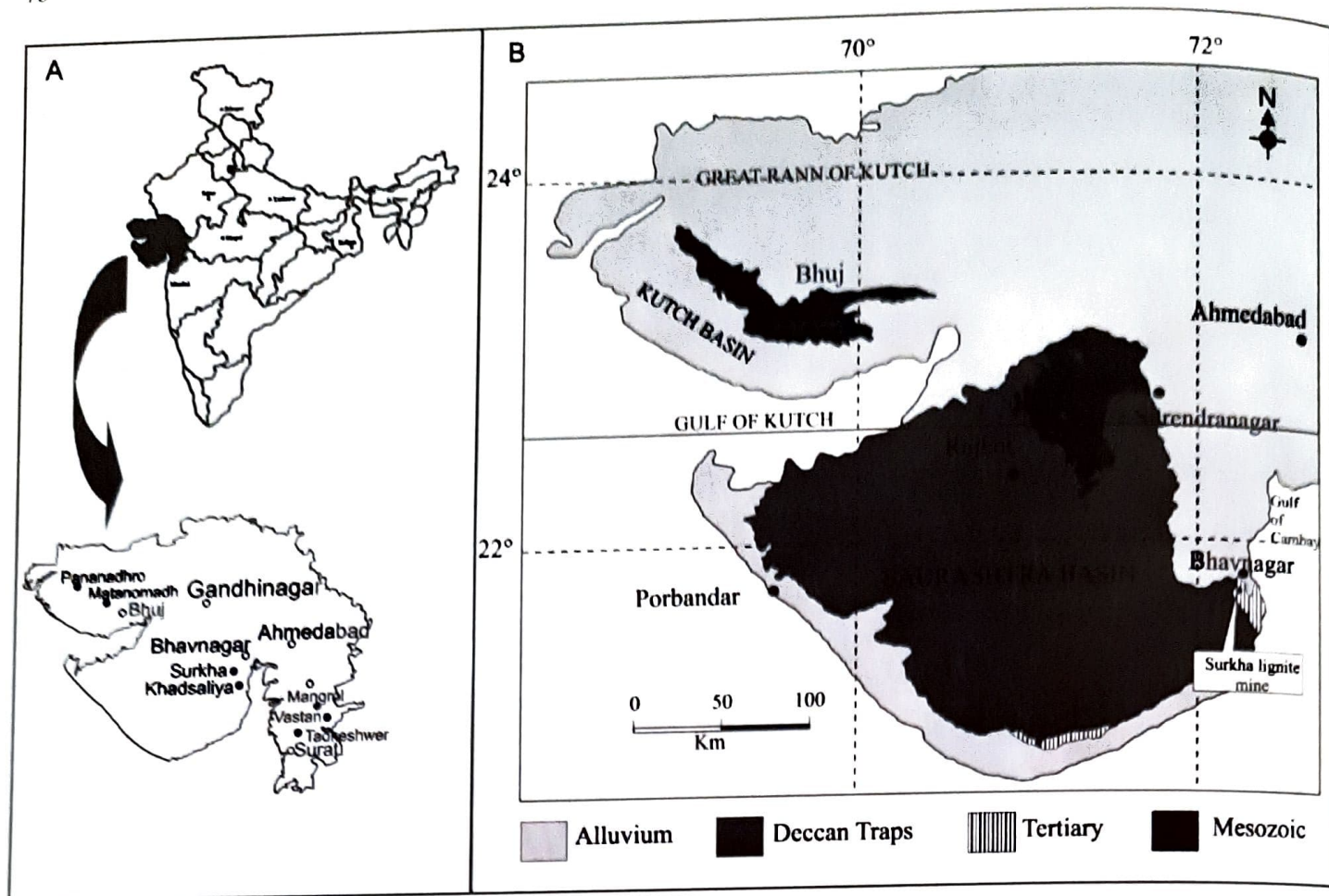
INTRODUCTION

Organic petrography is one of the most useful techniques to obtain information on nature (in terms of macerals), composition, rank or thermal maturity and mineral matter content of organic deposits (coals/lignites) for their assessment for various applications, using both reflected white light and fluorescence (blue light excitation) microscopy (Stach et al. 1982, Teichmüller 1989, Taylor et al. 1998, Suárez-Ruiz et al. 2012). Petrographic data derived from maceral analyses have been the subject of numerous studies to deduce the conditions under which the precursors of organic deposit originated (Suárez-Ruiz et al. 2012, Singh et al. 2013). The petrographic characteristics

reflect the environmental conditions during the accumulation of peat while coalification in turn points to the evolution of coal/lignite biomass precursors (Amijaya & Littke 2005).

In India, the lignite deposits are distributed in the Eocene (in Gujarat and Rajasthan), Miocene (Tamil Nadu and Kerala) and Plio-Pleistocene (Jammu and Kashmir) sedimentary sequences (Gowrisankaran et al. 1987, Singh et al. 2010). In Gujarat, lignite deposits are found within the Kachchh Basin (Kachchh District), Cambay Basin (Surat and Bharuch districts), and Saurashtra Basin (Bhavnagar District) (Text figure 1A).

The lignites from various mines of Gujarat have been investigated petrographically to characterize, and



Text figure 1. (A) Location map of Surkha lignite mine, Gujarat state, India. (B) Geological map of Saurashtra Basin (Modified after Merh 1995).

to deduce their depositional patterns (Misra 1992, Misra & Navale 1992, Singh 2002, Singh & Singh 2005, Thakur et al. 2010, Singh et al. 2010, Dutta et al. 2011, Singh et al. 2012, 2013). The present study deals with the organic petrographic characterization (maceral composition, rank and mineral matter content) of the Surkha lignite. The study area, Surkha lignite mine (latitude: $21^{\circ} 40' 24''$ N and longitude: $72^{\circ} 11' 71''$ E) exposing lignite deposits of Saurashtra Basin is situated about 20 km southeast of the city of Bhavnagar (Bhavnagar district) in Gujarat. The petrographically obtained data set are utilized to deduce depositional conditions of lignite-forming peat in the mire, and to know maturation trend of lignite and various related interpretations. The presently studied lignite has also been compared with the Khadsaliya lignite (Thakur et al. 2010) of the Saurashtra Basin to obtain an overall information on lignites of the basin.

GEOLOGICAL SETTING

The Surkha lignite mine in Gogha area of Bhavnagar District (Gujarat) is part of the Saurashtra peninsula, flanked by alluvial plains in the northeast. The peninsula is bounded by N–S orienting Cambay Basin fault in the east, the extension of Narmada geo-fracture (a fault system) in the south, E–W orienting gulf of Kachchh fault in the north, and the major WNW–ESE fault (an extension of the West Coast fault system in the Arabian Sea) in the west. About 65% of the Saurashtra peninsula is covered by basaltic lava flows (Deccan Trap), overlying the Mesozoic sediments in the north, and underlying the Tertiary-Quaternary sediments at coastal fringe (Merh 1995, Text figure 1B). The Deccan Trap provides the basement for the deposition of lignite-bearing Tertiary sediments that are exposed at some places. A general lithostratigraphic succession of the area is given in Table 1 (in accordance with GMDC 2008).

Table 1. Generalized lithostratigraphic succession in and around Gogha area, Saurashtra Basin (Modified after GMDC Report 2008).

Formation	Lithology	Age
Recent	Alluvial, coastal dunes and beach sand, mud flats, soil, etc.	Recent to sub-recent
----- Unconformity -----		
Lakhanka Formation (Agate Conglomerate Formation)	Agate, conglomerate and associated ferruginous sandstone with intercalation of clays	Pleistocene to sub-recent
----- Unconformity -----		
Piram Beds	Fossiliferous conglomerate grits and sandy clays	Upper Miocene to Pliocene
----- Unconformity -----		
Gaj Formation	Variegated sandstone, marl conglomerate, impure limestone and gypsum clays	Lower Miocene
----- Unconformity -----		
Khadsaliya Clays	Grey to greenish-grey clays with carbonaceous clay and lignite seams with siderite nodules	Eocene
----- Unconformity -----		
Supratrapean	Laterite, lithomerge, bentonite	Lower Eocene
----- Unconformity -----		
Deccan Trap	Basaltic lava flows with intrusive dykes	Cretaceous to Eocene

The Aravalli trend in the SW portion of the region splay out into three components (Biswas 1987, Merh 1995). The main NE–SW orientation trend continues across the Cambay Graben into Saurashtra as a south-westerly plunging arch. Biswas and Deshpande (1983) considered the Saurashtra region as a horst surrounded by rift graben and have demonstrated that the central, southern and northern Saurashtra exhibit distinct volcano-tectonic characteristics. On the eastern side of Saurashtra, a sharp contact of alluvium with basalt is observed in the N–S direction, extending from the west of Nal Sarovar to Bhavnagar.

LIGNITE DEPOSITS

The lignite in the area occurs in the Khadsaliya Clay Formation of Ypresian age (Paul et al. 2015). The formation, overlying the Supratrapean and Deccan Traps (Cretaceous-Eocene), holds the lignite seams along with carbonaceous clay. The lignite deposits unconformably lie on the weathered Trap on lithomargic clay. They become thicker towards east to north-east and diminish towards the sea. There are two lignite seams in the studied area measuring 0.50 m and about 12 m in thickness. The lignites are brownish-black in colour, soft, amorphous textured and fine grained, and

tend to develop cracks when dried. The lignite seams contain yellow resinous material and pyrite specks. The lignite seams in the area are not much affected by the structural disturbances, except for thinning out at some places. The lignite deposit at Surkha lignite mine is being mined by the Gujarat Mineral Development Corporation Limited (GMDC). Proximate analysis data of Surkha lignite mine (GMDC Report 2008) reveals that the moisture content is up to 42.50% ash content is 7.35%; volatile matter is 28.08%, and fixed carbon content is 22.06%. The calorific value of Surkha lignite is 3662 kcal/kg as specified in the GMDC report.

MATERIAL AND METHODS

A total of 18 lignite samples were collected from Surkha opencast mine following the channel sampling method. All the 18 samples were utilized for the petrographic investigation. The distribution of lignite samples in different seams are shown in Text figure 2. Polished particulate lignite pellets were prepared, by embedding $\pm 1-2$ mm size particles in a homogeneous mixture of epoxy resin and hardener in a ratio of 5:1 as per the ISO Standard (2009a). The hardened pellets were ground and polished successively on finer grades of Carbimet papers and silicon cloth with polishing alumina, respectively.

The maceral descriptions and terminologies as provided by the International Committee for Coal and Organic Petrology (ICCP) for huminite (Sýkorová et al. 2005), for liptinite (Taylor et al. 1998), and for inertinite (ICCP 2001) were followed. The analysis was performed following the ISO Standard (2009b). The maceral analysis was carried out on Leica DM4500P microscope, simultaneously under normal reflectance (incident light) and fluorescence (blue light excitation) modes by adopting the Single-Scan method, using oil immersion objective (50x). Quantitative estimation of macerals were made through automatic computerized point counter using 2.35 version of Petroglite software. Leica Applications Suit was used as a software tool for maceral images. For rank determination, the reflectance was measured on huminite (ulminite) maceral, following the ISO Standard (2009c), in monochromatic light using reflectance standards as Sapphire (0.594) and Yttrium-Aluminium-Garnet (0.904), and immersion oil (refractive

Table 2. Maceral composition (vol.%), mineral matter content (vol.%), huminite reflectance (R_r%) and petrographic indices of lignite from Surkha Lignite Mine.

Sample No.	BOTTOM SEAM												TOP SEAM							
	SN-1	SN-2	SN-3	SN-4	SN-5	SN-6	SN-7	SN-8	SN-9	SN-10	SN-11	SN-12	AVG.	SN-13	SN-14	SN-15	SN-16	SN-17	SN-18	AVG.
Macerals																				
Huminite(H)	53 (60)	43 (71)	60 (69)	64 (70)	63 (69)	56 (63)	44 (49)	64 (74)	64 (70)	64 (68)	61 (67)	49 (60)	57 (65)	54 (70)	56 (68)	65 (69)	58 (69)	63 (71)	72 (77)	61 (70)
Telohuminite	30	20	34	35	34	31	23	38	42	41	36	22	32	0	1	P	1	2	1	33
Textinite	3	0	2	2	P	1	2	2	2	1	1	1								
Ulminite	27	20	33	33	33	30	21	36	40	39	35	21		25	34	37	30	33	33	
Detrohuminitic	21	20	23	24	23	23	20	22	19	18	20	25	21	26	17	23	22	23	31	24
Attrinite	3	7	4	3	4	4	4	5	3	4	1	2		4	3	4	5	6	7	
Densinite	17	14	18	21	19	19	16	17	16	14	19	23	4	23	15	18	17	17	24	
Gelohuminite	2	3	3	5	7	2	1	4	4	5	6	3	4	2	3	5	5	6	7	5
Corpohuminite	2	3	3	5	7	2	1	4	4	5	6	3		2	3	5	5	6	7	
Gelinite	0	0	0	0	0	0	0	0	0	0	0	0		0	0	0	0	0	0	
Liptinite (L)	27 (31)	13 (22)	18 (20)	21 (23)	20 (22)	30 (34)	37 (40)	16 (19)	17 (19)	15 (16)	17 (19)	22 (27)	21 (24)	13 (16)	19 (23)	20 (21)	20 (23)	16 (18)	15 (15)	18 (20)
Sporinite	2	1	2	2	1	3	4	2	1	2	1	2		2	1	2	1	2	4	
Cutinite	2	1	P	1	1	2	1	1	2	1	2	2		P	2	2	2	1	2	
Suberinite	3	1	P	2	2	6	4	1	2	1	1	3		1	2	3	1	0	0	
Resinite	9	7	5	5	8	7	10	5	5	3	5	5		4	5	3	4	5	4	
Alginite	0	0	0	0	0	0	0	0	0	0	0	0		0	0	0	0	0	0	
Bituminite	1	0	2	0	1	1	1	3	2	2	1	0		0	0	0	1	1	0	
Fluorinite	1	P	0	1	0	1	1	0	1	P	1	1		0	0	P	1	0	0	
Exsudatinite	0	0	0	0	0	0	0	0	0	0	0	0		0	0	0	0	0	0	
Liptodetrinite	10	4	8	9	8	11	15	4	4	6	8	10		6	9	10	9	7	5	
Inertinite (I)	11 (14)	4 (7)	12 (11)	7 (7)	8 (9)	3 (3)	13 (16)	5 (7)	10 (12)	14 (15)	12 (14)	13 (14)	9 (10)	11 (14)	7 (9)	9 (10)	10 (12)	8 (9)	8 (9)	9 (10)
Semifusinite	2	1	2	1	P	1	2	P	P	3	2	P		1	P	0	1	0	0	
Fusinite	0	0	0	0	0	0	0	0	0	0	0	0		0	0	0	0	0	0	
Funginite	3	2	4	3	4	1	4	4	5	3	3	5		8	6	7	8	6	7	
Secretinite	0	0	0	0	0	0	0	0	0	0	0	0		0	0	0	0	0	0	
Macrinite	0	0	0	0	0	0	0	0	0	0	0	0		0	0	0	0	0	0	
Micrinite	0	0	0	0	0	0	0	0	0	0	0	0		0	0	0	0	0	0	
Inertodetrinite	6	1	6	4	5	1	7	3	6	8	7	8		2	1	2	1	2	1	
Mineral Matter (MM)	10	39	13	8	7	9	10	16	9	8	7	16	13	22	17	6	16	13	8	14
Others	8	35	8	7	4	4	5	8	4	5	3	13		6	7	4	7	8	6	
Pyrite	2	4	5	1	3	5	5	8	5	3	4	3		16	10	2	9	5	2	
Fluorescing H	17	8	15	16	15	14	10	15	16	13	17	17		12	13	12	14	14	12	
Non-fluorescing (H)	35	34	45	49	48	42	34	48	48	50	44	32		41	43	52	44	49	60	
Total Fluorescing (H+L)	46	23	32	36	37	46	46	31	33	28	37	41		26	33	33	33	30	26	
Non-fluorescing (H+I+M)	54	77	68	64	63	54	54	69	67	72	63	59		74	67	67	67	70	74	
R _r mean %	0.27	0.28	0.31	0.32	0.29	0.28	0.34	0.27	0.27	0.33	0.28	0.28	0.29	0.32	0.33	0.32	0.33	0.32	0.33	0.32
Gelification Index (GI)	3.1	3.3	3.5	4.8	4.8	6.5	2.4	4.3	3.8	2.9	3.9	3.3	3.9	3.5	4.6	4.6	4.0	3.5	4.1	4.0
Tissue Preservation Index (TPI)	1.3	1.0	1.5	1.5	1.5	1.4	1.0	1.7	1.9	1.9	1.6	0.8	1.4	0.9	2.0	1.6	1.4	1.5	1.2	1.4
Groundwater Index (GWI)	0.9	2.1	0.9	0.9	0.9	0.9	1.0	0.8	0.6	0.6	0.9	1.9	1.0	1.6	0.9	0.7	1.0	0.9	0.9	1.0
Vegetation Index (VI)	1.1	1.0	1.1	1.0	1.1	1.1	0.8	1.3	1.5	1.3	1.1	0.7	1.1	0.8	1.4	1.1	1.0	1.0	0.9	1.0

index: 1.518). Microscope photometer system—PMT III and Software MSP 200 was used for the random reflectance (R_{mean}) measurements and data calculations.

RESULTS

Maceral Composition:

The frequency distribution of various macerals and associated mineral matter in studied Surkha lignites is shown in Table 2 and Text figure 3. The representative microphotographs of certain macerals are illustrated in Plate 1.

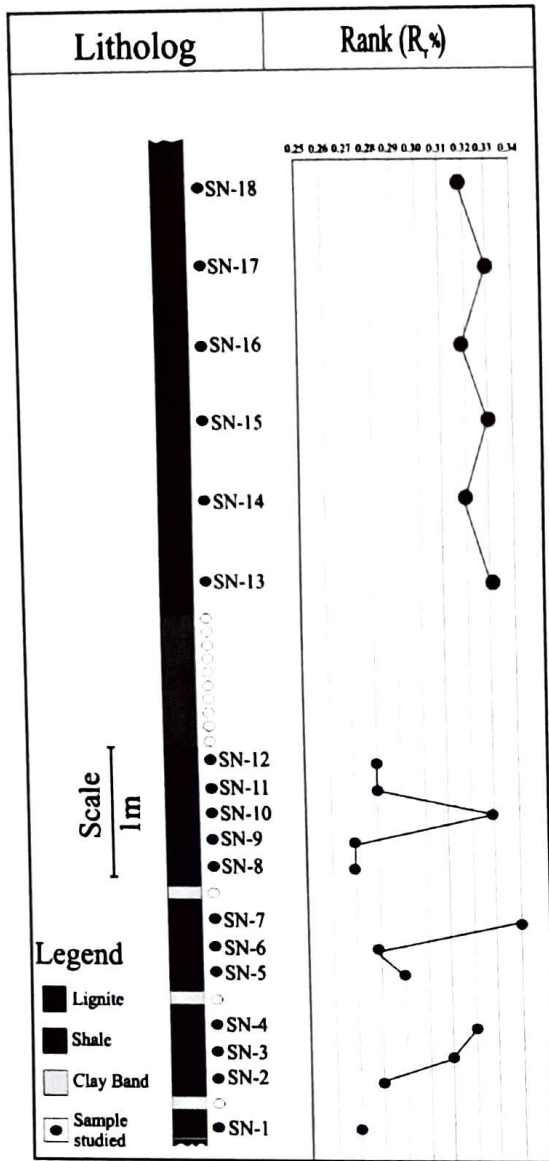
Huminite Group: The lignite of the top seam has relatively higher content (53-72 vol. %, avg. 61 vol. %) of huminites than that of the bottom seam (42-

64 vol. %, avg. 57 vol. %). Almost all the lignite seams are rich in huminite content (42-72 vol. %, avg. 61 vol. %). Huminites are predominantly composed of structured telohuminite (textinite + ulminite: avg. 31 vol. %), which shows dominance in both the seams and ranges between 19 to 42 vol. % in the bottom seam, and between 25 to 37 vol. % in the top seam. Ulminite is the main constituent of telohuminite; that varies between 19 to 42 vol. %. The detritus detrohuminite (attrinite + densinite) is the subdominant maceral in the top seam (18-31 vol. %, avg. 24 vol. %) however, its frequency is slightly lower in the bottom seam (17-25 vol. %, avg. 21 vol. %). Detrohuminite is chiefly represented by the maceral densinite in both the seams



Plate 1

Representative photographs of macerals in Surkha lignites. (in reflected white light), A) ulminite, B-C) textinite, D) corpohuminite, E) inertodetrinite in huminite groundmass, F) attrinite and densinite (right portion), G) cluster of funginite, H-I) pyrite framboids and crystals, (in fluorescence mode) J) cluster of sporinite, K) cutinite (surface view), L) thick-walled cutinite, M) suberinite, N) resinite bodies, O) resinite (cell fillings), P) liptodetrinite, Q) cutinite (Cu) associated with fluorinite (Fl) and resinite (R), R) bituminite impregnated in huminite.



Text figure 2. Litholog of Surkha mine showing the distribution of lignite seams and rank variations in the studied samples.

(bottom: 14-23 vol. %, top: 15-24 vol. %). Gelohuminite, i.e., the gelified huminite, is mainly represented by corpohuminite in both the seams (bottom: 1-7 vol. %, top: 2-7 vol. %).

Overall, the concentration of huminite group is almost similar throughout the seams with a slightly increasing tendency towards the top. The fluorescing fractions of the huminite group fluoresce are dark reddish-brown or brown in colour (with low intensity). These fluoresce is either due to relics of cellulose and/or by resinous impregnations in huminite. The amount of perhydrous (or fluorescing) huminite is almost same in both the seams (bottom: 8-17 vol. %, avg. 14 vol. %; top: 12-14 vol. %, avg. 13 vol. %). No definite trend in the distribution of perhydrous huminite has been

observed in the studied lignite seams. As it is well represented in all the samples throughout the seams.

Liptinite Group: The liptinites are represented by sporinite (spores-pollen), cutinite (cuticles), resinite (resins/waxes/latex etc.), suberinite (cork and bark cells), fluorinite (essential oils), and liptodetrinite (detritus). These macerals appear relatively darker to black in normal incident light, as compared to macerals of huminite. Liptinites tend to fluoresce under blue light excitation in different colours and intensities, and hence, are easily recognized under fluorescent light and by their distinct morphographic features. These fluoresce in yellow, greenish-yellow, yellowish-brown to brown colours. The liptinites are well represented in both the seams. The total liptinite content in the studied lignite seams varies between 14 and 36 vol. % (avg. 20 vol. %) with relatively higher proportion in the bottom seam (15-36 vol. %, avg. 22 vol. %) as compared to that of the top seam (14-21 vol. %, avg. 17 vol. %). In both the seams, liptinites are represented chiefly by liptodetrinite (bottom: 4-15 vol. %, top: 5-10 vol. %) and resinite (bottom: 3-10 vol. %, top: 3-5 vol. %), followed by sporinite (bottom: 1-4 vol. %, top: 1-3 vol. %), suberinite (bottom: 0-6 vol. %, top: 0-3 vol. %) and cutinite (0-2 vol. %).

Resinite incorporates the oil secretions and resins, the metabolic products of plants, and is found as discrete bodies of various shapes and sizes and as cell fillings. Liptodetrinite includes the relics and fragmented parts of liptinite macerals which had lost their identity. Bituminite (0-3 vol. %) and fluorinite (0-1 vol. %, associated with cutinite) are sporadic. Bituminite is mostly accounted for the perhydrous huminite.

Inertinite Group: The inertinite group (avg. 8 vol. %) in order of abundance is mainly represented by funginite, inertodetrinite and semifusinite. Funginite varies between 1 and 5 vol. % in the bottom seam, and between 5 to 7 vol. % in the top seam. Inertodetrinite varies from 1 to 8 vol. % in the bottom seam, and 1 to 3 vol. % in the top seam. Semifusinite is not present in all the samples and is poorly represented in both the seams (up to 1 vol. %). A transition from huminite to semifusinite has been observed in some of the samples. Greyish-white semifusinite is characterized by well-

preserved cell structures. Funginite, characterized by single and multi-celled fungal spores (teleutospores) and as oval and elliptical bodies (fungal sclerotia), is common. It is well represented in both the seams, however, with higher range (5-7 vol.%) in the top seam. Inertodetrinite is represented by fragmentary pieces of semifusinite and funginite. Amongst the three maceral groups, the inertinite group is recorded in lowest concentration in the lignite seams (bottom: 3-14 vol.%, top: 6-11 vol.%) with no definite trend in its distribution.

Mineral Matter:

The studied Surkha lignites contain an appreciable amount of mineral matter (avg. 13 vol.%) ranging between 7 to 16 vol.% in the bottom seam, and between 6 to 16 vol.% in the top seam. Two samples (nos. SN-2, SN-13) in the seams show higher amount (more than 20%) of mineral matter contents. Sample no. SN-2, just above the clay band of bottom seam, shows the highest mineral matter content (39 vol.%). The mineral inclusions are represented by clastic (clay and quartz) and sulphide (pyrite) minerals along with the sporadic presence of carbonate minerals (siderite and calcite). The clastic minerals (bottom seam: 3-13 vol.%, top seam: 4-8 vol.%) occur as granules, lumps and bands that intimately associated with almost all the macerals. Pyrite has been recorded in fine crystalline and massive as well as in concretionary and framboidal forms (Plate-1 H, I), with higher concentration in the top seam (2-16 vol.%) than that of the bottom seam (1-8 vol.%). In the top seam, pyrite is also found in association with globular resinite as embedded framboids. The highest mineral content in SN-2 is mainly due to higher clastic minerals in this sample (35 vol.%) since the pyrite in this sample is recorded within the normal range.

Perhydrous huminite and all the macerals of liptinite group form the fluorescing contents in Surkha lignites. Fluorescing (perhydrous huminite + liptinites) and the non-fluorescing (huminites + inertinites + mineral matter) contents vary between 23 to 46 vol.% (avg. 36 vol.%), and between 54 to 77 vol.% (avg. 64 vol.%) in the bottom seam. The top seam has a relatively higher concentration of non-fluorescing (range 67-74 vol.%, avg. 70 vol.%) and lower concentration (range 26-33 vol.%, avg. 30 vol.%) of fluorescing contents as compared to the bottom seam.

Palaeomire Conditions:

Maceral analysis (type, nature and amount of macerals) has significance in elucidating the peat-forming environmental conditions of the organic deposits. The petrographic indices viz., gelification index (GI), tissue preservation index (TPI), groundwater index (GWI) and vegetation index (VI) derived from maceral compositions have been used to depict the depositional environment during the peat accumulation (Diessel 1986, Calder et al. 1991, Kalkreuth et al. 1991, Lamberson et al. 1991, Kalaitzidis et al. 2000, Flores 2002, Mavridou et al. 2003, Amijaya & Littke 2005 and others).

Diessel (1986) originally developed TPI and GI for high rank Australian Permian coals which were later modified by Kalkreuth et al. (1991) and Kalaitzidis et al. (2000) for low rank coals/lignites. TPI is the ratio of structured to non-structured macerals, indicating the degree of humification of the peat-forming materials. High TPI values (>1) either indicate fast subsidence of the basin or the dominance of wood-derived tissues. Low TPI values (<1), however, suggest slow subsidence rate of the basin with enhanced humification or the predominance of herbaceous vegetation in the palaeomires (Diessel 1992). TPI also indicates pH conditions of palaeomires because, in a low pH condition, microbial activity is weak and plants can be well preserved, and vice-versa (Zhang et al. 2010). The TPI of the studied lignites has been calculated as per the following equation:

$$\text{TPI} = (\text{telohuminite} + \text{corpohuminite} + \text{fusinite} + \text{semifusinite}) / (\text{atrinite} + \text{densinite} + \text{gelinite} + \text{inertodetrinite})$$

GI is the ratio of gelified components to non-gelified components, indicating the wet or dry conditions during the peat accumulation. Higher GI values (>1) indicate wet mire conditions, whereas, the dry condition is indicated by lower GI value (<1). The GI has been calculated as per the following equation:

$$\text{GI} = (\text{ulminite} + \text{Gelohuminite} + \text{densinite}) / (\text{textinite} + \text{atrinite} + \text{inertinite})$$

Calder et al. (1991) proposed a palaeo-environmental model based on GWI and VI indices of

Pennsylvanian coal from Canada. The GWI indicates the level of ground water (and relative rainfall) during the peat accumulation as mires are usually formed in successive variations between rheotrophic and ombrotrophic hydrological conditions (Amijaya & Littke 2005, Silva et al. 2008). The GWI values less than 0.5 indicate ombrotrophic hydrological conditions, whereas, values more than 1.0 indicate rheotrophic hydrological conditions and values in between these are indicative of the mesotrophic hydrological condition. Kalaitzidis et al. (2000) modified the formula for lignite by adding gelinite and densinite macerals in the numerator, as both are suggestive of higher water level (and relatively wet conditions), and attrinite in the denominator as attrinite forms in drier conditions than densinite (Mavridou et al. 2003). The GWI of the studied Surkha lignites has been calculated as per the following equation:

$$\text{GWI} = (\text{corpohuminite} + \text{gelinite} + \text{densinite} + \text{mineral matter}) / (\text{textinite} + \text{ulminite} + \text{attrinite})$$

The VI is related to the type of vegetation that dominated the mire. It is dependent on the type of peat-forming plant communities and is indicative of the type of vegetation (e.g., trees and shrubs). The VI of the studied lignites has been calculated as per the following equation:

$$\text{VI} = (\text{telohuminite} + \text{resinite} + \text{suberinite} + \text{fusinite} + \text{semifusinite}) / (\text{detrohuminite} + \text{inertodetrinite} + \text{cutinite} + \text{sporinite} + \text{alginite} + \text{bituminite} + \text{liptodetrinite})$$

The GI, TPI, GWI and VI values for the Surkha lignites are represented in Table 2.

Rank of Lignites:

Random reflectance values of huminite (ulminite) are used to determine the rank (or thermal maturity) of lignites. The calculated mean ($R_{r\text{mean}}$) values range from 0.27 to 0.34% (avg. 0.29%) for the bottom seam, and from 0.32 to 0.33% (avg. 0.32%) for the top seam (Table 2, Text figure 2). The reflectance values indicate that the Surkha lignites have attained 'brown coal' (German Standard) or 'lignite' stage/rank (Stach et al. 1982) or can be classified as 'Low rank B (Lignite B)' as per ISO-11760 (2005) and fall in the early diagenetic zone of methane generation (Taylor et al. 1998). The

top seam shows a relatively higher reflectance value in comparison to the bottom one, which can be attributed to the increased frequency of funginite associated with huminite (Belkin et al. 2010). The enzymes secreted by fungi augment the decomposition of woody remains, and this event can be attributed to the enhanced reflectance of huminite (Hower et al. 2009) of the top seam.

COMPARISON WITH KHADSALIYA LIGNITE

The comparison between presently studied Surkha lignites and Khadsaliya lignites of the same basin (Thakur et al. 2010) indicate that these are almost similar in their petrographic composition; predominantly composed of huminite followed by liptinite and inertinite macerals. The Khadsaliya lignites, however, have relatively higher liptinite and lower content of inertinite as compared to those of Surkha lignites. The lower values of inertinite in Khadsaliya lignites are indicative of less arid condition during peat accumulation and/ or faster subsidence of the basin than that of the Surkha mine. A marked difference in the contents of fluorescing huminite has been found in lignites of two mines. The top and bottom lignite seams of these mines possess inverse proportion of this maceral (Surkha– bottom: avg. 14%, Khadsaliya– bottom: avg. 8%; Surkha– top: avg. 13%, Khadsaliya– top: avg. 3%). The total fluorescing content is very high in the top seam of Khadsaliya mine (almost double the amount in Surkha mine), however, it is almost similarly represented in the bottom seams of both the mines. The difference in frequencies may be due to higher liptinites content in the top seam of Khadsaliya mine.

The lignites from both the mines have good potential for the generation of hydrocarbons, as indicated by high total fluorescing contents. Lignites of both the mines are similar with respect to their maturation because both possess almost similar rank values (Surkha: average $R_{r\text{mean}}$ 0.30%, Khadsaliya: average $R_{r\text{mean}}$ 0.29%).

DISCUSSION

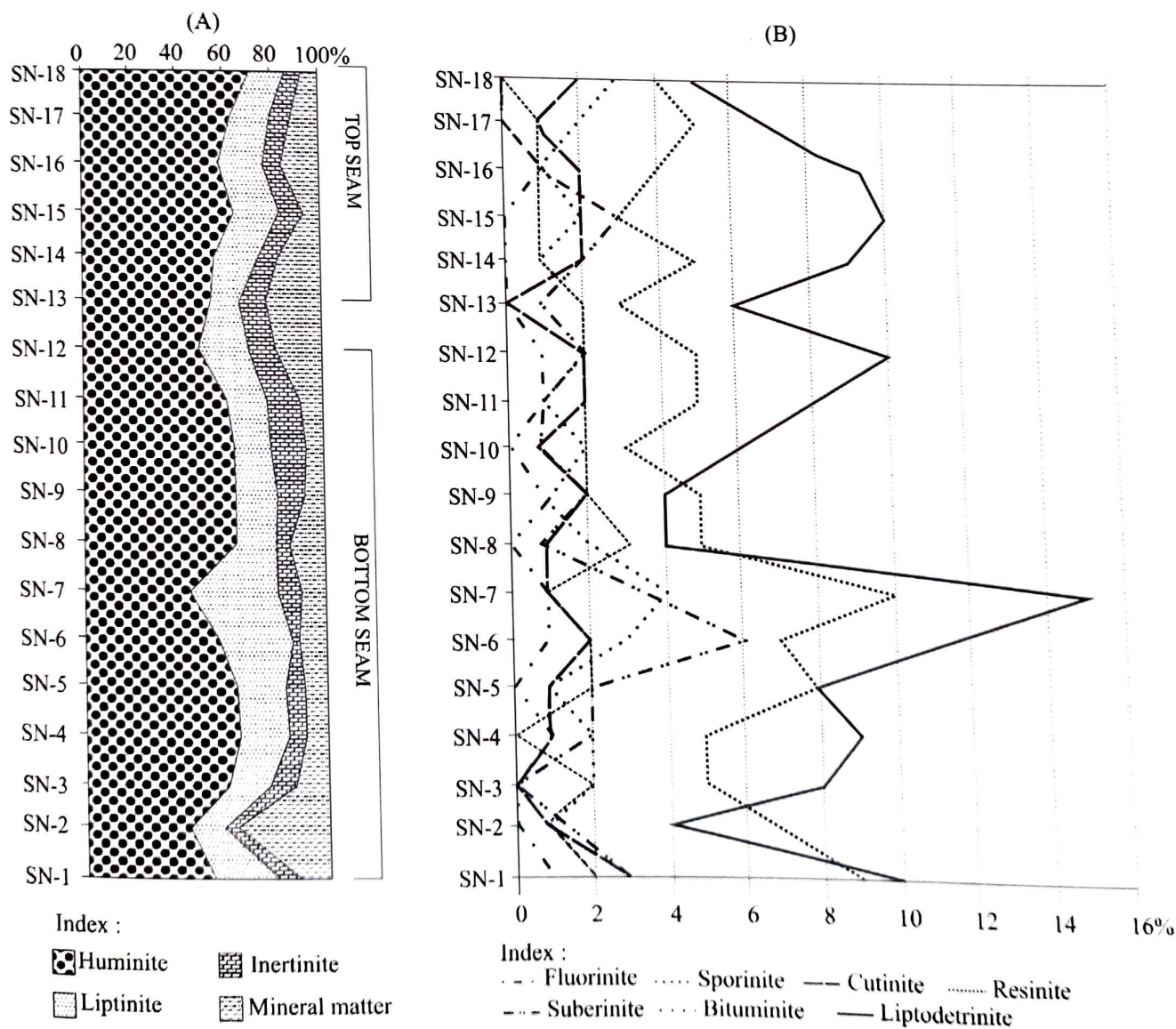
The petrographic composition of Surkha lignites reveals the predominance of huminite maceral followed by liptinite and inertinite group macerals. The

predominance of huminite group macerals indicates the woody forest/vegetation (lignin- and cellulose-rich tissues; Stach et al. 1982, Teichmüller 1989, Taylor et al. 1998) as the main source for the formation of Surkha lignites in the Saurashtra Basin. Fair proportions of resinite, suberinite, sporinite, and cutinite in the studied lignites (Table 2, Text figure 3B) suggest that hinterland vegetation was dominated by higher plants during the time of peat accumulation. High frequency of resinite and suberinite indicates the dominance of resin secreting arboreal plants i.e., angiosperms and mangroves (Singh et al. 2013).

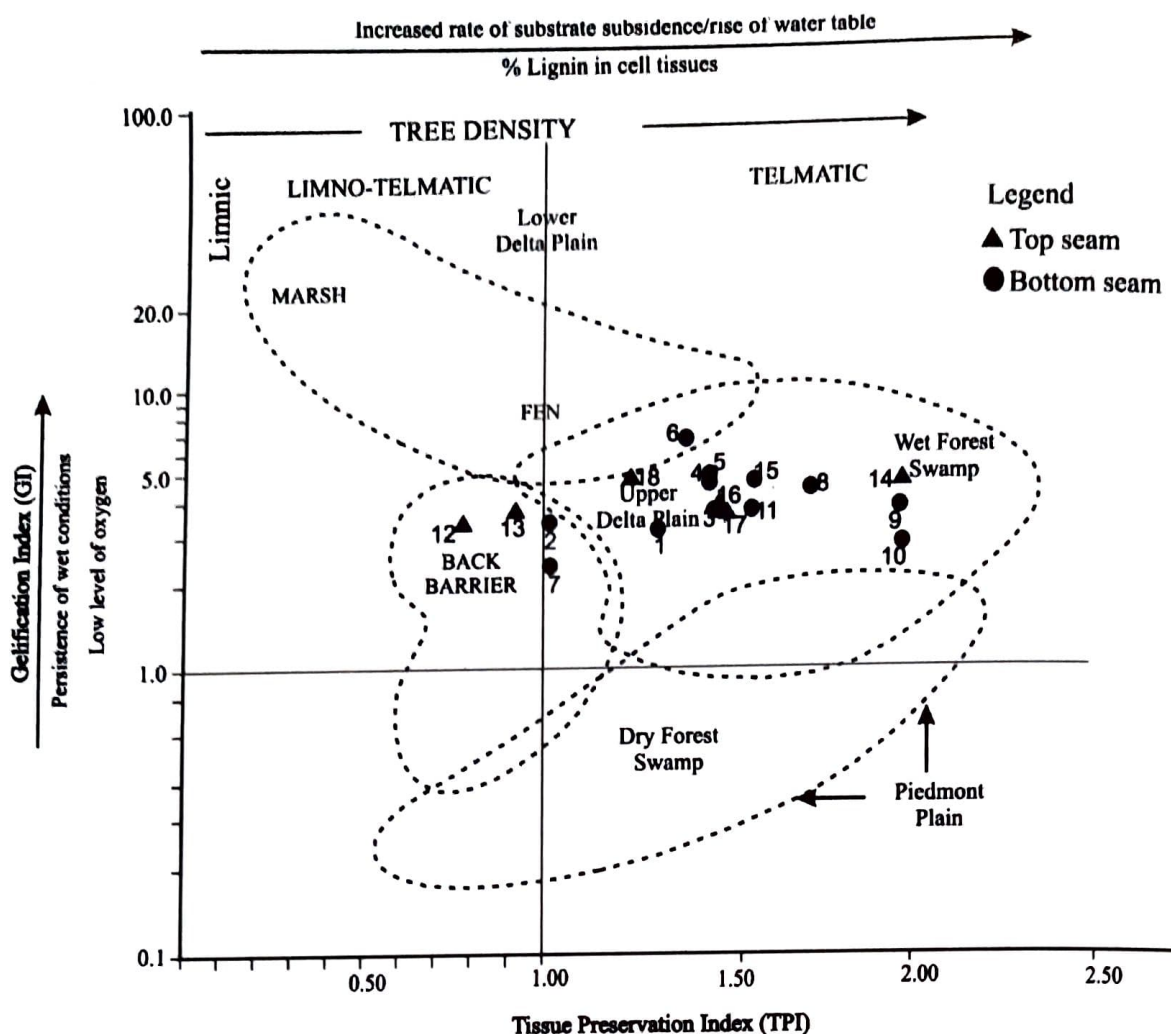
The presence of non-arboreal/herbs, shrubs and pteridophytes is evidenced by the appreciable amount of detrohuminite in these lignites. Their occurrence is

indicative of contribution of soft woody tissues from the herbaceous and pteridophytic plants as a source, which tends to decompose easily and give rise to attrinite and densinite. So, it can be assumed that herbs and shrubs including pteridophytes also grew profusely, in and around the basin during early Eocene time, as undergrowth in the dense woody forests (angiospermic and back mangroves). Their presence is also corroborated by plant mega- and microfossil records from the basin (Guleria 1991, Samant 2000).

The GI and TPI values for the Surkha lignites are plotted on the facies diagram (Text figure 4) following Diessel (1992). A moderate to high TPI values (0.9-2.0) of lignites suggest the dominance of woody plants in the peat-forming biomass. The GI values (2.4-4.8)



Text figure 3. Maceral composition: (A) Cumulative frequency of maceral groups. (B) Relative distribution of selective liptinite macerals in the studied Surkha lignites.



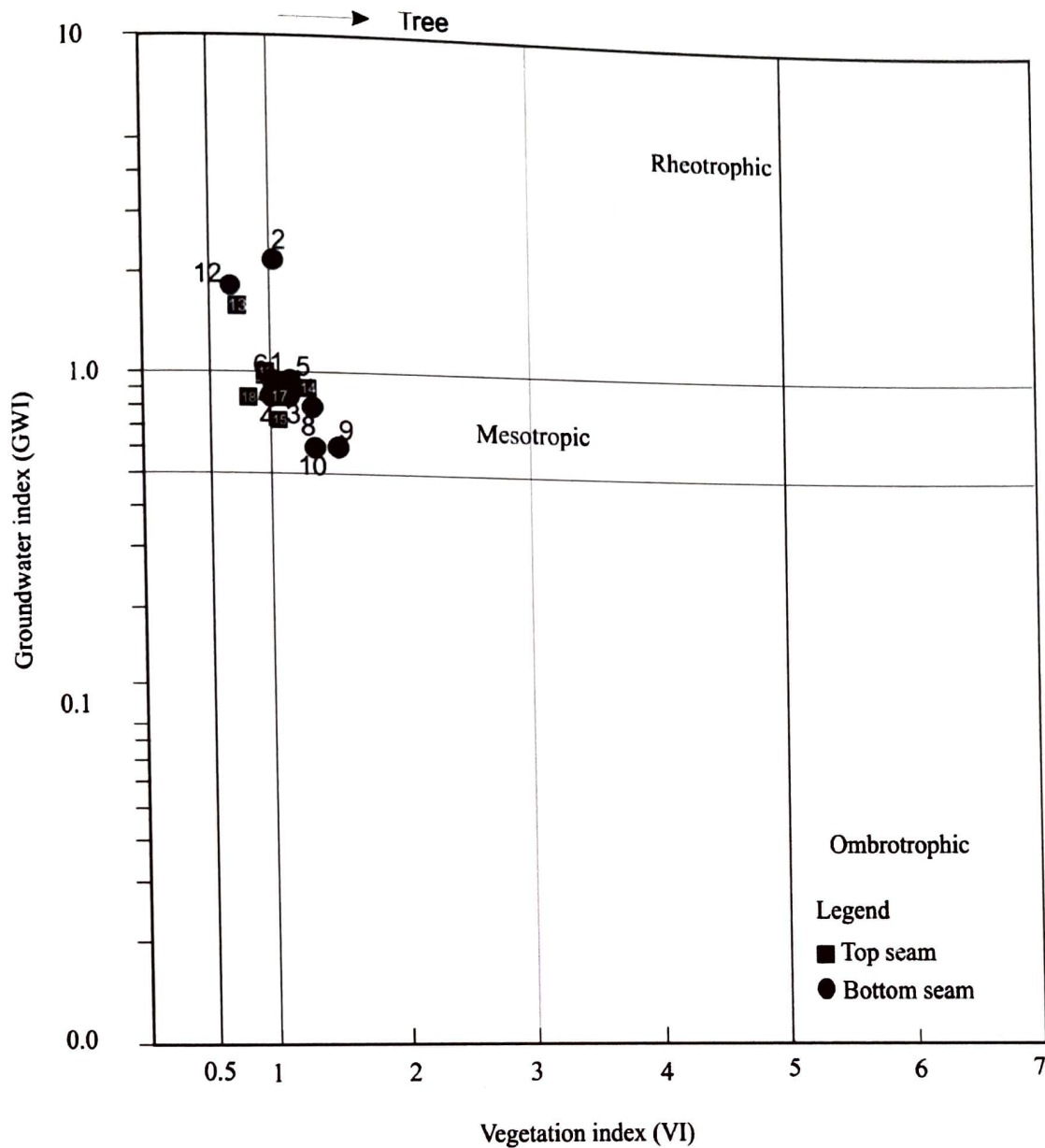
Text figure 4. Facies diagram in terms of GI and TPI in relation to depositional setting and type of mire for Surkha lignites.

together with the high huminite content suggest wettest conditions of mires during the development of peat. The GWI and VI values for the studied lignites are also plotted on the palaeoenvironment diagram (Text figure 5) following Calder et al. (1991). The GWI values (0.9-2.1) indicate mesotrophic to rheotrophic hydrological conditions during the peat accumulation. The VI values (0.8-1.5) reflect the dominance of woody plant community with sub-dominance of herbaceous sub-aquatic vegetation.

The GI-TPI and GWI-VI facies models suggest that the precursor of peat was deposited mainly in upper deltaic regime (with occasional limno-telmatic conditions) under the mesotrophic hydrological regime. However, sample nos. SN-2, SN-12 and SN-13 indicate rheotrophic hydrological regime; suggesting fluctuating hydrological conditions of palaeomires during the peat formation. High contents of telohuminate (mainly

ulminite) in both the seams reflect that the depositional site witnessed exuberant vegetation represented by higher plants, which contributed for the woody tissues. The depositional site was well fed by the fluvial source, which resulted in the gelification and preservation of tissues. Low VI and a fair amount of detrohuminite along with the other dominating maceral of huminite indicate the contribution of herbaceous/bushy plants as a source material, as they decompose easily.

The cross plot of ulminite and detrohuminite shows an inversely proportional trend with respect to their frequency in the lignites (Text figure 6). The distribution reflects the hydrological state of mires, wherein the increase in ulminite content with the corresponding decrease in detrohuminite is due to the submerged mire with high water table. The reversal of ulminite-detrohuminite frequencies indicates a low water table or draining out of mire water. Shifting mineral matter

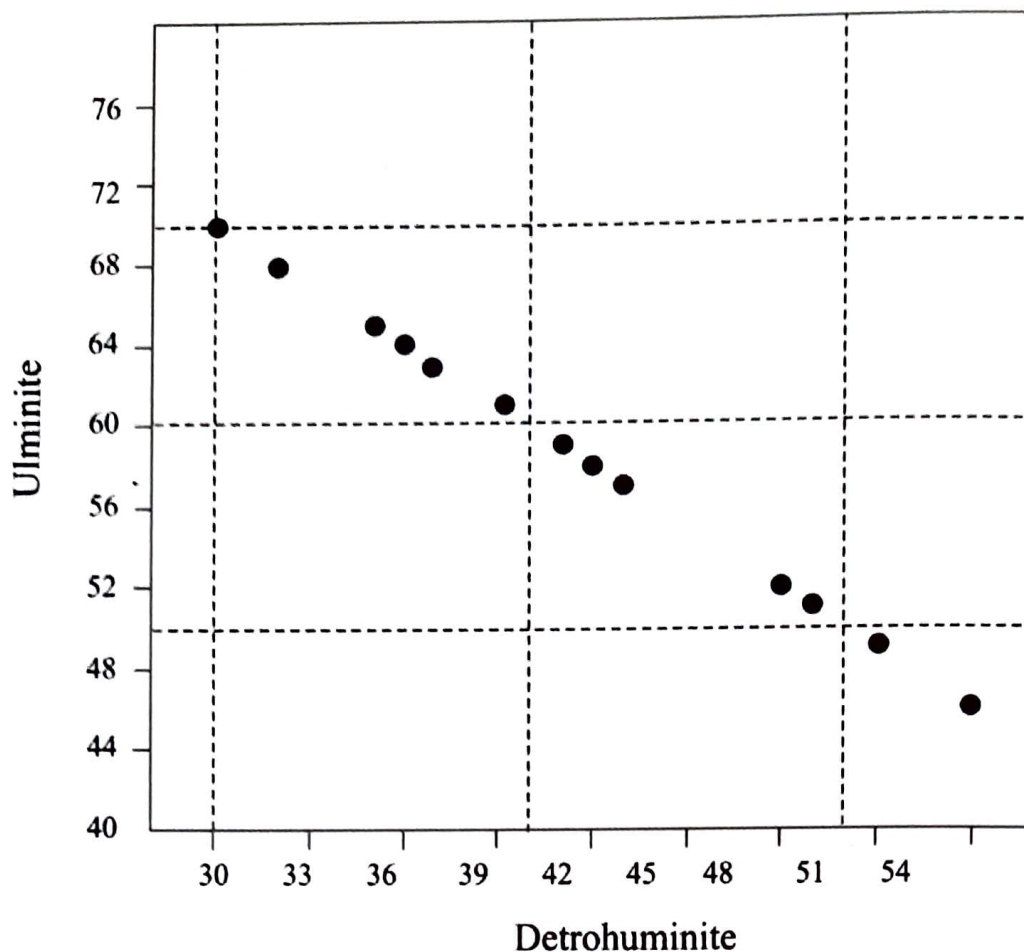


Text figure 5. Palaeoenvironment diagram using GWI and VI indices of Surkha lignites.

contents in the bottom seam suggests the high standing water table in the mire, inundated by sediment-laden waters. A high percentage of detrohuminite in the upper part of the top seam may be due to the influx of oxygenated water (sea water), thereby facilitating the augmented degradation of organic matter which added to the frequency of detrohuminite. This is further supported by the increased pyrite contents in the top seam, due to high sulphur availability and high influx of oxygenated water during its accumulation (Petersen & Ratanasthien 2011).

Low content of textinite and high amount of liptodetrinite reflect the anaerobic decomposition of organic matter and high pH conditions of swamp water. Severe bacterial degradation of organic matter is also

evident from the presence of framboidal pyrites. The decomposition products of liptinite get perfused in the huminite, forming perhydrous or fluorescing huminite (Taylor et al. 1998) which is appreciably represented in both the lignite seams. Low content of inertinite macerals suggests that the peat surface witnessed an occasional aerial exposure either due to fast subsidence or receding water table for a short period of time. The relatively higher percentage of funginite maceral (of inertinite group) in the studied lignites, indicates warm and humid/ moist climatic conditions during the time of peat accumulation. Such conditions favour for the growth of fungi and also for the luxuriant vegetation. Moderate to the high association of pyrite (up to 16%, including framboidal) in the lignites suggests bacterial



Text figure 6. Cross-plot of ulminite and detrohuminite contents of Surkha lignites.

degradation of organic matter and marine incursion (brackish-water influence) during the deposition of peat.

The average values and vertical frequency distribution of macerals, mineral matter; petrographic indices and rank values indicate that both top and bottom lignite seams are almost similar with respect to their origin, depositional conditions and maturation. Minor fluctuations in peat-forming biomass, depositional conditions and maturation are, however, reflected by slight vertical frequency variations of macerals, petrographic indices and rank values. The bottom seam is less mature as compared to that of the top seam. Approximately one meter thick shale band sandwiched between top and bottom seams indicate non-conductive conditions for the deposition of peat-forming biomass. Extermination of bottom lignite seam due to mineral influx is evident from the high mineral contents in samples SN-12 and 13. The formation of shale band occurred due to the paucity of organic matter/vegetal matter and abundance of mineral matter, probably due to floods.

The conditions slowly became conducive for the formation of lignite in the top seam.

The petrographic characteristics of Surkha lignites indicate their amenability for utilization in industries for the generation of steam/heat. In addition, the presence of perhydrous huminite and hydrogen-rich liptinites (23-46%, Table 2) in the lignites, which are the progenitors of hydrocarbons (Singh & Singh, 2008), indicate their potentiality for hydrocarbon generation. The macerals of liptinite group (sporinite, cutinite, suberinite, resinite, liptodetrinite, etc.) are recognized as belonging to visual kerogen type II. These macerals, along with perhydrous huminite (with hydrogen-rich aliphatic edge group on humic substance) have potential to generate aliphatic hydrocarbons (oil/gas). The macerals of huminite group, which are predominant in the studied lignites, as a whole, belong to kerogen type III (gas prone) and indicate their potential for gas generation. Thus, good prospects of hydrocarbon generation, both for oil and gas, in the studied lignites are evident.

CONCLUSION

The early Eocene lignite seams encountered in Surkha mine of Saurashtra Basin has been analyzed in terms of their maceral composition and rank. Lignites are rich in huminite group of macerals (mainly ulminite and densinite) followed by liptinite (chiefly resinite and liptodetrinite) and inertinite (mainly funginite and inertodetrinite) group macerals, along with low to moderately high associated mineral matters. Reflectance values of huminite indicate that lignites occur in the early diagenetic zone of methane generation.

The predominance of woody tissues-derived huminite group macerals indicates that the studied lignites were formed from woody forests/vegetation (including herbs and shrubs), and the deposition took place in sub-aqueous, anaerobic environmental conditions in a fast subsiding basin with only minor fluctuations in swamp water conditions. High proportions of detrohuminite (attrinite and densinite) in the lignites suggest a predominance of herbaceous plants in the palaeomires which are prone to bacterial degradation in slow subsiding palaeomires. High amounts of telohuminite (ulminite and textinite) indicate the predominance of forest plants in rapidly subsiding palaeomires. The limno-telmatic environment during the deposition of lignite seams is indicated by the petrographic indices (GI-TPI and GWI-VI). The depositional site or palaeomire experienced fluctuating hydrological conditions between mesotrophic and rheotrophic regimes. Moderate pyrite content in the studied lignites suggests marine incursions during peat accumulation. Evidently, the deposition of Surkha lignite seams took place in deltaic regime (upper delta plain) under brackish water influence with the prevalence of humid tropical conditions. In addition, fair amounts of hydrogen-rich macerals (visual kerogen type II/ type III) indicate their potential for the hydrocarbons (oil and gas) generation.

Based on overall petrographic characterization it can be concluded that both the Surkha and Khadsaliya lignites of the Saurashtra Basin are broadly similar in terms of their depositional environment.

ACKNOWLEDGEMENTS

Authors thank the Director of the Institute for permitting (BSIP/RDCC/39/2013-14) to publish the paper. One of us (V.P.S.) is indebted to the authorities of Birbal Sahni Institute of Palaeobotany for providing Birbal Sahni Research Scholarship. Thanks are also due to the officials of GMDC at Ahmedabad and Surkha lignite mine for their kind support and help during the field visit. The assistance of Mr. V.P. Singh, Technical Officer of the Institute, in sample preparation is also thankfully acknowledged.

REFERENCES

- Amijaya H. & Littke R. 2005. Microfacies and depositional environment of Tertiary TanjungEnim low rank coal, South Sumatra Basin, Indonesia. *International Journal of Coal Geology* 61: 197-221.
- Belkin H.E., Tewalt S.J., Hower J.C., Stucker J.D., O'Keefe J.M.K., Tatu C.A. & Buia G. 2010. Petrography and geochemistry of Oligocene bituminous coal from the Jiu Valley, Petroani basin (southern Carpathian Mountains), Romania. *International Journal of Coal Geology* 82: 68-80.
- Biswas S.K. 1987. Regional tectonic framework, structure and evolution of the western marginal basins of India. *Tectonophysics* 135: 302-327.
- Biswas S.K. & Deshpande S.V. 1983. Geology and hydrocarbon prospect of Kutch, Saurashtra and Narmada basins. *Petroleum Asia Journal* 6: 111-126.
- Calder J.H., Gibling M.R. & Mukhopadhyay P.K. 1991. Peat formation in a Westphalian B piedmont setting, Cumberland Basin, Nova Scotia: Implications for the maceral-based, interpretation of rheotrophic and raised paleomires. *Bulletin of the Geological Society of France* 162(2): 283-298.
- Diessel C.F.K. 1986. On the correlation between coal facies and depositional environments. *Proc. 20th Symp. Geol. Dept. Univ. Newcastle, NSW, Australia*, pp. 19-22.
- Diessel C.F.K. 1992. *Coal Bearing Depositional Systems*. Springer-Verlag, Berlin, pp.721.
- Dutta, S., Mathews R.P., Singh B.D., Tripathi S.K.M., Singh A., Saraswati P.K., Banerjee S. & Mann U. 2011. Petrology, palynology and organic geochemistry of Eocene lignite of Matanomadh, Kutch Basin, western India: Implications to depositional environment and hydrocarbon source potential. *International Journal of Coal Geology* 85: 91-102.
- Flores D. 2002. Organic facies and depositional palaeoenvironment of lignites from Rio Maior Basin (Portugal). *International Journal of Coal Geology* 48: 181-195.
- GMDC 2008. Gujarat Mineral Development Corporation, Mine report. (<http://www.gmdcltd.com/projects/lignite-projects/bhavnagar.aspx>).
- Gowrisankaran S., Sethi P.P., Hariharan R. & Agarwal K.P. 1987. Lignite deposits of India- their occurrences, depositional features and characteristics. In: R.M. Singh (ed.), *Proc. Nat. Sem. Coal Res. India, Varanasi*, pp. 481-553.

- Guleria J.S. 1991. On the occurrence of carbonized woods resembling *Terminalia* and *Sonneratia* in Palaeogene deposits of Gujarat, western India. *Palaeobotanist* 39: 1-8.
- Hower J.C., O'Keefe J.M.K., Watt M.A., Pratt T.J., Eble C.F., Stucker J.D., Richardson A.R. & Kostova I.J., 2009. Notes on the origin of inertinite macerals in coals: Observations on the importance of fungi in the origin of macrinite. *International Journal of Coal Geology* 80: 135-143.
- ICCP (International Committee for Coal Petrology) 2001. The new inertinite classification (ICCP System 1994). *Fuel* 80: 459-471.
- ISO (2009a) Methods for the petrographic analysis of bituminous coal and anthracite– Part 2: Methods of preparing coal samples. International Organisation for Standardization, ISO, Geneva, 8.
- ISO (2009b) Methods for the petrographic analysis of bituminous coal and anthracite– Part 3: Methods of determining maceral group composition. International Organisation for Standardization, ISO, Geneva, 4.
- ISO (2009c). Methods for the petrographic analysis of bituminous coal and anthracite– Part 5: Methods of determining microscopically the reflectance of vitrinite. International Organisation for Standardization, ISO, Geneva, 11.
- ISO- 11760. 2005. Classification of coals. International Standard, 1-9.
- Kalaitzidis S., Bouzinos A. & Christanis K. 2000. Paleoenvironment of lignite formation prior to and after the deposition of the "characteristic sand" in the lignite deposit of Ptolemais. *Miner Wealth, Athens* 115: 29-42.
- Kalkreuth W.D., Marchioni D.L., Calder J.H., Lamberson M.N., Naylor R.D. & Paul J. 1991. The relationship between coal petrography and depositional environments from selected coal basins in Canada. *International Journal of Coal Geology* 19: 21-76.
- Lamberson M.N., Bustin R.M. & Kalkreuth W. 1991. Lithotype (maceral) composition and variation as correlated with paleowetland environment, Gates Formation, Northeastern British Columbia, Canada. *International Journal of Coal Geology* 18: 87-124.
- Mavridou E., Antoniadis P., Khanaqa P., Riegel W. & Gentzis T. 2003. Paleoenvironmental interpretation of the Amynteon-Ptolemaida lignite deposit on northern Greece based on its petrographic composition. *International Journal of Coal Geology* 56: 253-268.
- Merh S.S. 1995. *Geology of Gujarat*. Geological Society of India, Bangalore, pp. 222.
- Misra B.K. & Navale G.K.B. 1992. Panandhro lignite from Kutch (Gujarat), India: Petrological nature, genesis, rank and sedimentation. *Palaeobotanist* 39: 236-249.
- Misra B.K. 1992. Spectral fluorescence analysis of some liptinite macerals from Panandhro lignite (Kutch), Gujarat, India. *International Journal of Coal Geology* 20: 145-163.
- Paul S., Sharma J., Singh B.D., Saraswati P.K., Dutta S. 2015. Early Eocene equatorial vegetation and depositional environment-biomarker and palynological evidences from a lignite-bearing sequence of Cambay Basin, western India. *International Journal of Coal Geology* 147: 7-92.
- Petersen H.I. & Ratanasthien B. 2011. Coal facies in a Cenozoic paralic lignite bed, Krabi Basin, southern Thailand: Changing peat-forming conditions related to relative sea-level controlled water table variations. *International Journal of Coal Geology* 87: 2-12.
- Samant B. 2000. Palynostratigraphy and age of the Bhavnagar lignite, Gujarat, India. *Palaeobotanist* 49: 101-118.
- Silva M.B., Kalkreuth W. & Holz M. 2008. Coal petrology of coal seams from the Leão- Butiá Coalfield, Lower Permian of the Paraná Basin, Brazil-Implications for coal facies interpretations. *International Journal of Coal Geology* 73: 331-358.
- Singh A. & Singh B.D. 2005. Petrology of Panandhro lignite deposit, Gujarat in relation to palaeodepositional conditions. *Journal Geological Society of India* 66: 334-344.
- Singh A. & Singh B.D. 2008. Progenitors of hydrocarbons in Indian coals and lignites and their significance. *Memoirs of Geological Society of India* 71: 117-133.
- Singh A. 2002. Rank assessment of Panandhro lignite deposit, Kutch Basin, Gujarat. *Journal Geological Society of India* 59: 69-77.
- Singh A., Mahesh S., Singh H., Tripathi S.K.M. & Singh B.D. 2013. Characterization of Mangrol lignite (Gujarat), India: Petrography, palynology, and palynofacies. *International Journal of Coal Geology* 120: 82-94.
- Singh A., Thakur O.P. & Singh B.D. 2012. Petrographic and depositional characteristics of Tadkeshwar lignite deposits (Cambay Basin), Gujarat. *Journal Geological Society of India* 80: 329-340.
- Singh B.D., Singh A., Thakur O.P. & Mahesh S. 2013. Petrological evaluation of Tertiary lignites from Amod Mine (Bharuch District), Gujarat. *International Journal Applied Engineering Research* 8: 111-116.
- Singh P.K., Singh M.P. & Singh A.K. 2010. Petro-chemical characterization and evolution of Vastan lignite, Gujarat, India. *International Journal of Coal Geology* 82: 1-16.
- Stach E., Mackowsky M.-Th., Teichmüller M., Taylor G.H., Chandra D. & Teichmüller R. 1982. *Stach's text book of Coal Petrology*. 3rd edition, Gebrüder Borntraeger, Stuttgart, pp. 535.
- Suárez-Ruiz I., Flores D., Mendonça Filho J.G. & Hackley P.C. 2012. Review and update of the applications of organic petrology: Part 1, geological applications. *International Journal of Coal Geology* 99: 54-112.
- Sókorová I., Pickel W., Christanis K., Wolf M., Taylor G.H. & Flores D. 2005. Classification of huminite– ICCP System 1994. *International Journal of Coal Geology* 62: 85-106.
- Taylor G.H., Teichmüller M., Davis A., Diessel C.F.K., Littke R. & Robert P. 1998. *Organic Petrology*. Gebrüder Borntraeger, Berlin, pp. 704.
- Teichmüller M. 1989. The genesis of coal from viewpoint of coal petrology. *International Journal of Coal Geology* 12: 1-87.
- Thakur O.P., Singh A. & Singh B.D. 2010. Petrographic characterization of Khadsaliya lignites, Bhavnagar District, Gujarat. *Journal Geological Society of India* 76: 40-46.
- Zhang S., Tang S., Tang D., Pan Z. & Yang, F. 2010. The characteristics of coal reservoir pores and coal facies in Liulin district, Hedong coalfield of China. *International Journal of Coal Geology* 81: 117-127.